DEVELOPMENTAL DYNAMICS 235:3456–3465, 2006

Cloning and Expression Pattern of Chicken *Ror2* and Functional Characterization of Truncating Mutations in Brachydactyly Type B and Robinow Syndrome

Sigmar Stricker,[1,2]* Nicole Verhey van Wijk,[1,2] Florian Witte,[1,2] Norbert Brieske,[1] Kathrin Seidel,[1] and Stefan Mundlos[1,2]

Ror2 is a receptor tyrosine kinase mutated in the human syndromes Brachydactyly type B (BDB) and recessive Robinow syndrome (RS). In this study, we used the chick as a model to investigate the role of Ror2 in skeletogenesis and to elucidate the functional consequences of *Ror2* mutations. For this purpose, we cloned chicken *Ror2* and analyzed its expression pattern at various embryonic stages by in situ hybridization and immunolabeling. We document expression of *cRor2* in several organs, including mesonephros, heart, nervous system, intestine and cartilage. The high conservation of expression when compared with the mouse underlines the validity of the chick as a model system. Using replication-competent retroviral vector–mediated overexpression, we analyzed the functional consequences of truncating BDB and RS mutations in the developing chick limb. Overexpression of Ror2 mutants led to a disturbance of growth plate architecture and a severe block of chondrocyte differentiation, demonstrating the functional importance of Ror2 in skeletogenesis. *Developmental Dynamics 235:3456–3465, 2006.*

Key words: Ror2; Brachydactyly; Robinow syndrome; limb development; cartilage; chicken

Accepted 21 September 2006

INTRODUCTION

Mammalian Ror2 and the closely related paralog Ror1 belong to a small family of receptor tyrosine kinases (RTKs) that have been characterized by their homology to MuSK and Trk-RTKs (Masiakowski and Carroll, 1992; Valenzuela et al., 1995). Ror2 possesses an intracellular tyrosine kinase domain and a C-terminal proline–serine–threonine—rich (PST) domain. In its extracellular part, Ror2 has an immunoglobulin-like domain, a cysteine-rich domain showing high homology to frizzled receptors (Saldanha et al., 1998) and a kringle domain. *Ror2* orthologs have been found in *Drosophila melanogaster* (Wilson et al., 1993; Oishi et al., 1997), *Caenorhabditis elegans* (Forrester et al., 1999), *Aplysia californica* (McKay et al., 2001), *Xenopus laevis* (Hikasa et al., 2002), *Mus musculus* (Oishi et al., 1999), and *Rattus norvegicus* (Masiakowski and Carroll, 1992; Katoh and Katoh, 2005).

Expression of *Ror2* has been extensively studied in the mouse. In the early embryo, *Ror2* is expressed in neural crest cells, neural tube, and primitive streak. Later, *Ror2* is expressed in limb buds, mandibular arches, the otic capsule, and the telencephalon. After organogenesis, *Ror2* shows a widespread expression and is found in the nervous system, in developing heart and lung, in the urogenital system and also in cartilage (Al-Shawi et al., 2001; Matsuda et al., 2001).

[1]Max Planck-Institute for Molecular Genetics, Development and Disease Group, Berlin, Germany
[2]Institute for Medical Genetics, University Medicine Charité, Berlin, Germany
Grant sponsor: Deutsche Forschungsgemeinschaft; Grant number: SFB 577.
***Correspondence to: Sigmar Stricker, Max Planck Institute for Molecular Genetics, Development and Disease Group, Ihnestr. 73, 14195 Berlin, Germany. E-mail: strick_s@molgen.mpg.de**

DOI 10.1002/dvdy.20993
Published online 23 October 2006 in Wiley InterScience (www.interscience.wiley.com).

Ror2 is an orphan receptor, and little is known about the pathway(s) it activates. There is accumulating evidence that Ror2 is implicated in Wnt signaling. In *Xenopus*, XRor2 is involved in the regulation of convergent extension, where it acts in synergy with the noncanonical XWnt11/silberblick (Hikasa et al., 2002). In mouse, Ror2 interacts with Wnt5a, thereby signaling by means of the noncanonical JNK-pathway (Oishi et al., 2003; Mikels and Nusse, 2006). Additionally, Ror2 has been implicated in Gdf5/BmpR1b signaling (Sammar et al., 2004).

The function of Ror2 has been elucidated by the finding that distinct truncating mutations in human *ROR2* can cause Brachydactyly type B (BDB, MIM 113000; Oldridge et al., 2000; Schwabe et al., 2000). BDB is a human limb malformation syndrome characterized by hypoplasia and/or aplasia of distal phalanges. Furthermore, mutations in *ROR2* are causative for a very distinct syndrome, autosomal recessive Robinow syndrome (RS, MIM268310; Afzal et al., 2000; van Bokhoven et al., 2000). RS is characterized by short stature, mesomelic limb shortening, hemivertebrae, genital hypoplasia, and characteristic facial features (Patton and Afzal, 2002).

Further insights into the functions of Ror2 came from loss-of-function studies in the mouse. Homozygous deficiency of Ror2 results in perinatal death with severe cyanosis. Overall, the Ror2-null embryos show multiple features overlapping with human RS (Schwabe et al., 2004). Concordantly it has been suggested that RS mutations result in loss of function, whereas BDB mutations act as dominant-negative proteins. Recently, it has been shown that RS mutations in the extracellular part of ROR2 lead to retention of the protein in the endoplasmic reticulum, thus leading to a loss of function (Chen et al., 2005).

Ror2-null mice show a variety of skeletal defects, including craniofacial abnormalities and a shortening of long bones, especially in the limb zeugopod (Takeuchi et al., 2000). Mice expressing a truncated Ror2-lacZ fusion protein additionally exhibit loss of medial phalanges (DeChiara et al., 2000). In cartilage, *Ror2* is expressed in cartilaginous condensations and throughout the growth plate. Additional expression is seen in the perichondrium and periosteum (DeChiara et al., 2000; Schwabe et al., 2004). Loss of Ror2 leads to a decrease of chondrocyte differentiation and delay of ossification, thus leading to mesomelic limb shortening (Schwabe et al., 2004).

Here we report the cloning and embryonic expression pattern of chicken *Ror2*. As the chicken is a widely used model system in developmental biology, we investigated the role of Ror2 in this system by retroviral overexpression of truncated forms of cRor2 corresponding to human mutations in recessive Robinow syndrome and Brachydactyly type B.

RESULTS AND DISCUSSION

Cloning of Chicken *Ror2*

Expressed sequence tag (EST) clone 369c3 containing the partial coding sequence for *cRor2* was obtained from the BBSRC (Boardman et al., 2002). Using whole chicken embryo day 5 (Hamburger and Hamilton stage [HH] 27) cDNA and genomic DNA, we cloned the full-length coding sequence (cds) of *cRor2* with a combination of degenerate reverse transcriptase-polymerase chain reaction (RT-PCR), genomic walking, and rapid amplification of cDNA ends (RACE). The *cRor2* cds consists of 2,805 nucleotides, compared with 2,835 in mouse (Oishi et al., 1999) and 2,832 in human (Masiakowski and Carroll, 1992). The deduced amino acid sequence of cRor2 shows a high degree of sequence identity with mouse and human (83.5% and 85.8%, respectively). The main differences are found in the leader peptide sequence. The extracellular domains as well as the intracellular TK and PST domains are highly conserved (Fig. 1A). In a phylogenetic tree derived from a multisequence alignment using all available vertebrate Ror2 sequences and *D. melanogaster* Ror as an outgroup, cRor2 is appropriately positioned between *X. laevis* Ror2 and the mammalian Ror2 group (Fig. 1B). To preclude influences of the divergent signal peptide sequences, an alignment without the signal peptides was done, which resulted in an identical tree.

Embryonic Expression of cRor2

The embryonic expression of the *Ror2* gene has been extensively studied in the mouse, but so far no expression pattern for a nonmammalian vertebrate *Ror2* has been described in detail. To gain an overall insight into the expression of *cRor2*, we first performed whole-mount in situ hybridization (WMISH). At HH23–27, we found expression of *cRor2* in the dorsal root ganglia (Fig. 2A–D, arrows), the branchial arches, craniofacial mesenchyme, and the otic vesicle (arrowheads). Overall, the expression pattern showed a high overlap with the expression seen in the mouse at comparable stages (Matsuda et al., 2001). Vibratome sections at HH25 demonstrated expression of *cRor2* predominantly in the dorsal–lateral layers of the dorsal root ganglia (drg, Fig. 2E,F). Section ISH also revealed expression of *cRor2* in dorsal–medial layers of the drg (Fig. 2G). Strong expression was also seen in the limb buds (Fig. 2H,I). In early limb buds, the expression of *cRor2* was detected all over the limb bud, with stronger expression in anterior and posterior areas. At later stages, the expression of *cRor2* in central mesenchyme was further weakened, while the expression in the anterior and posterior margins of the limb stayed intense, a pattern also observed in the mouse (Matsuda et al., 2001). Vibratome cross-sections demonstrated strong expression of *cRor2* in mesenchymal cells directly beneath the ectoderm in the trunk dermomyotome and in the limbs but not within the ectoderm (Fig. 2J).

To gain insight into the expression of cRor2 during organogenesis, we analyzed the distribution of cRor2 mRNA and protein on embryonic HH29 (day 6) sections. Specificity of signals was confirmed by using a sense probe for *cRor2*, which yielded no signal (not shown). We found expression of *cRor2* mRNA in a variety of organs (Fig. 3A,B). Strongest expression was seen in the nervous system. Signals were detected in the spinal chord and in the dorsal root ganglia (Fig. 3G,H). In the head, *cRor2* was expressed in the cerebral vesicle, the optic lobe, the nasal sac,

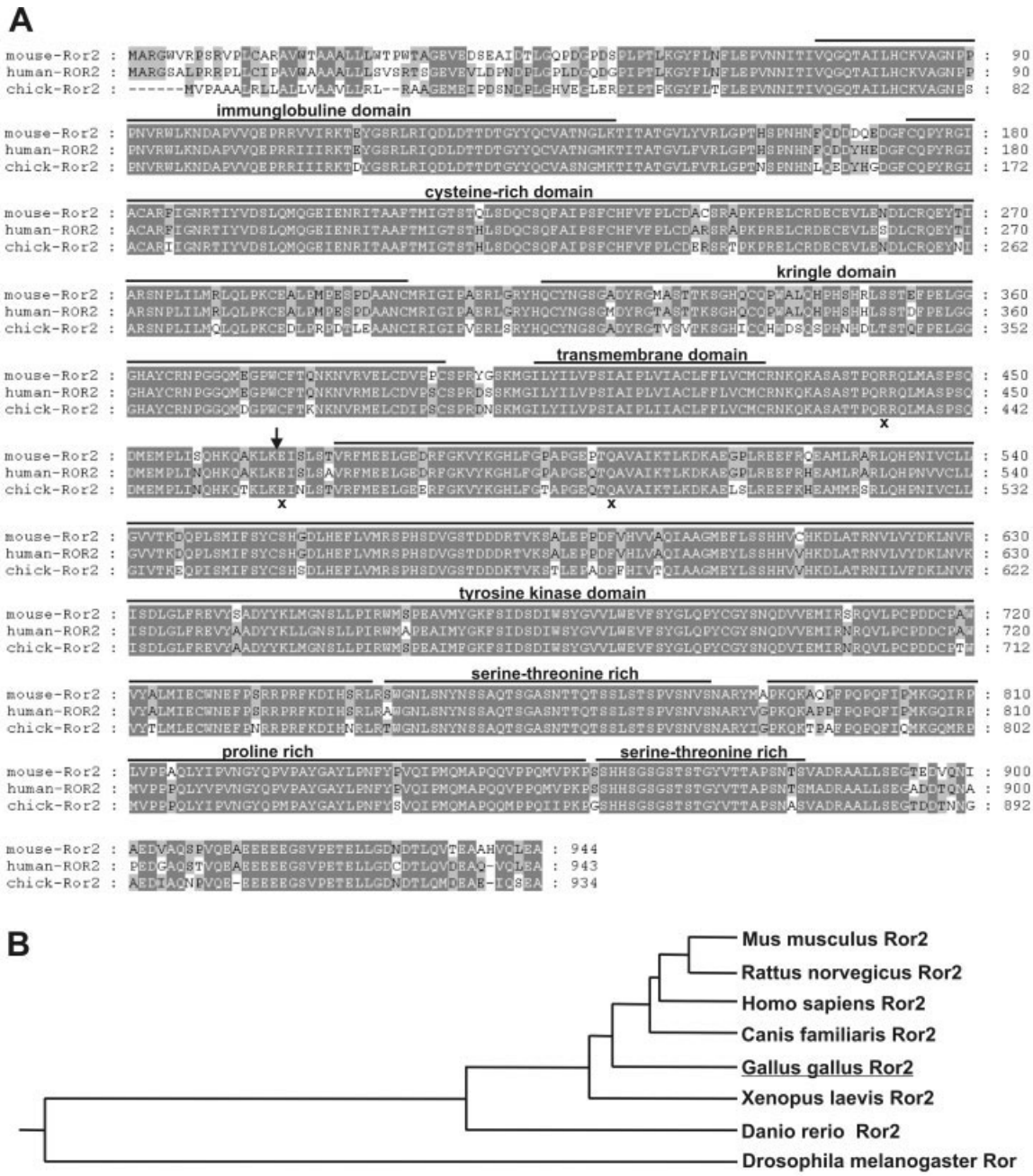

Fig. 1. **A:** Alignment of *Gallus gallus* (chicken) Ror2 with *Homo sapiens* (human) and *Mus musculus* (mouse) Ror2. Conserved amino acids between the three species are shaded black, and conserved amino acids between only two species are shaded gray. Positions of Brachydactyly type B (BDB) and Robinow syndrome (RS) mutations used in this study are indicated by an "x" below the alignment. Position where the human 1398insA frameshift was fused to the chicken sequence (at position 1374) is indicated by an arrow. **B:** Phylogenetic tree from an alignment of the Ror sequences indicated. Accession numbers: *Mus musculus*, BAA75481; *Rattus norvegicus*, XP_225181; *Homo sapiens*, Q01974; *Canis familiaris*, XP_541309; *Xenopus laevis*, AB087137; *Danio rerio*, XP_689681; *Drosophila melanogaster*, Q24488.

and Meckel's cartilage (Fig. 3K). Additional strong expression was observed in the otic vesicle, the basilar plate, the acoustic ganglion, and the cochleovestibular ganglion (Fig. 3K,L). We also detected *cRor2* in muscles, such as limb muscles and myocardium (Fig. 3A,C). In the digestive system, *cRor2* showed strong expression in the gizzard (Fig. 3D) and in the intestinal loops (Fig. 3I, arrows). Expression was also seen in the liver (Fig. 3D, arrowhead) and in the lung (Fig. 3J, arrows). Chicken *Ror2* was also detected in the mesonephric tubules (Fig. 3F). Additionally, we found *cRor2* expression in the cartilaginous condensations of the ribs (Fig. 3E, arrow).

For the immunolabeling on HH29 sections, anti-human ROR2 (R&D Systems) was used, which gave a clear signal for the chick Ror2 constructs, but no cross-reactions on Western blots made from chicken cell extracts (see Fig. 5B). The antibody staining largely confirmed the in situ hybridizations. Chicken Ror2 protein was

found in the heart (Fig. 3M), the gizzard (Fig. 3N), and the intestine (Fig. 3O). In the mesonephric tubules, the protein was predominantly localized to the tubular lumen (Fig. 3P). Expression of cRor2 was also confirmed in liver, lung, and dorsal root ganglia (Fig. 3Q–S).

Overall, the expression pattern of chicken *Ror2* is strikingly similar to the expression of *Ror2* in the mouse (Al-Shawi et al., 2001; Matsuda et al., 2001; Schwabe et al., 2004). Thus there is a high evolutionary conservation of the embryonic expression pattern of *Ror2*, indicating functional conservation. This finding makes the chick a valuable model for functional analysis of Ror2.

Human mutations in ROR2 as well as the inactivation of Ror2 in the mouse lead to severe defects in limb development. As the chicken is an important developmental model system and is frequently used for studying limb development, we analyzed the expression of *cRor2* in this process. As shown above, in the early limb bud, *cRor2* is expressed in superficial limb mesenchyme. As the differentiation of limb mesenchymal cells proceeds, different lineages of tissues arise within the limb, such as tendons, connective tissue and cartilage. At HH27, *cRor2* could be detected in the early cartilaginous condensations of the proximal skeletal elements of stylopod and zeugopod (Fig. 4A), while shortly after at HH30, it was also expressed in the condensations of the autopod (Fig. 4B). In all cases, the presumptive joints are excluded from *cRor2* expression.

The initial cartilaginous condensations of the limb skeleton start to expand by proliferation and undergo a series of differentiation steps ultimately resulting in the formation of hypertrophic cartilage. In a process called endochondral ossification, hypertrophic cartilage is eventually degraded and becomes replaced by bone. The tight regulation of proliferation on one hand and differentiation on the other ensures the proper shape and growth of the skeletal anlagen until they reach their final size. During this process, expression of *cRor2* was observed throughout the area of undifferentiated chondrocytes, but was excluded from hypertrophic cartilage (Fig. 4C). Additionally, we performed section ISH on E15.5 mouse limbs to compare the expression of *cRor2* in the growth plate to the expression in the mouse. As in the chick, *mRor2* was expressed strongly in all chondrocytes, except hypertrophic cartilage (Fig. 4D). This finding was also corroborated by lacZ staining on forelimbs of $Ror2^{lacZ/+}$ mouse embryos (DeChiara et al., 2000) (Fig. 4E). Overall, expression of *Ror2* in cartilaginous condensations of the ribs and the limb cartilage elements has been found in the mouse in a pattern equal to what we observed in the chick (Schwabe et al., 2004), confirming the evolutionary conservation of *Ror2* expression as we have observed it in other organs.

Skeletal Defects Caused by Overexpression of Truncated Ror2 Variants

Skeletal malformations are a major finding in RS (mesomelic limb shortening, hemivertebrae) as well as in BDB (missing phalanges). To gain insight into the functional consequences of the truncating mutations in both conditions on limb cartilage development, we used the RCAS replication competent retrovirus. We chose three different mutations that in humans lead to either BDB or RS. All mutations truncate the protein within a range of approximately 60 amino acids C-terminal of the transmembrane domain. We generated four different constructs (Fig. 5A). Two mutations in chick *Ror2* truncated the protein at positions corresponding to two different human BDB mutations (Schwabe et al., 2000) by introducing a stop codon. However, human mutations at these sites result in frameshifts, adding additional amino acids to the polypeptide until a premature stop is reached. Thus we made a chimeric construct carrying the human frameshift caused by the 1398insA mutation (Schwabe et al., 2000) fused to the chicken *Ror2* sequence at the corresponding position (c/hRor2 1374insA). The fourth mutation (Q494X) truncates the protein at a position identical to the human RS mutation Q502X (Afzal et al., 2000). As cloning into the RCAS virus is limited to a maximal size of approximately 2.4 kb (Morgan and Fekete, 1996), the further C-terminal truncations causing BDB and RS or the full-length wild-type *cRor2* could not be used in this system. All truncated variants of *cRor2* in RCAS are strongly expressed when transfected into chicken DF-1 cells. Proteins were of correct size and were stable (Fig. 5B).

To analyze the functional consequences of truncating mutations in Ror2 in vivo and to get an insight into the function of Ror2 in the chick, we overexpressed the different mutant constructs in developing chicken limbs. RCAS–green fluorescent protein was used as a control and elicited no effect on limb patterning and outgrowth (not shown). To assess the function of mutant Ror2, the truncated constructs were injected into HH10 forelimb or hindlimb fields, which yields high infection throughout the limb mesenchyme. First, embryos were harvested after a total of 7 days of incubation (HH32). At that time, the proximal skeletal elements of the limbs are already established and start to differentiate, while the cartilaginous elements of the autopod are still in the process of condensation. When the embryos were harvested at this early stage, overexpression of the different constructs resulted in comparable phenotypes, thus representative data are shown for construct E459X only (Fig. 6A). Overexpression of truncated forms of Ror2 has no obvious effect on skeletal patterning, but the cartilage elements in the wing as well as in the leg appear shorter and thicker when compared with the uninfected contralateral control limbs. Of interest, the proximal elements of the zeugopod and stylopod were more severely affected than the autopod. Humerus and femur were affected most severely, with the femur showing a reduction in size of up to 70%.

Concomitant with the onset of hypertrophic differentiation and ossification, functional differences between the different mutants became apparent. Figure 6B shows representative examples from injections of the truncated constructs harvested at day 11 of development (HH37; $n > 8$ for each). Overall, the strongest effects were observed for the BDB mutations E459X and 1374insA. In both cases, the differentiation of the cartilaginous

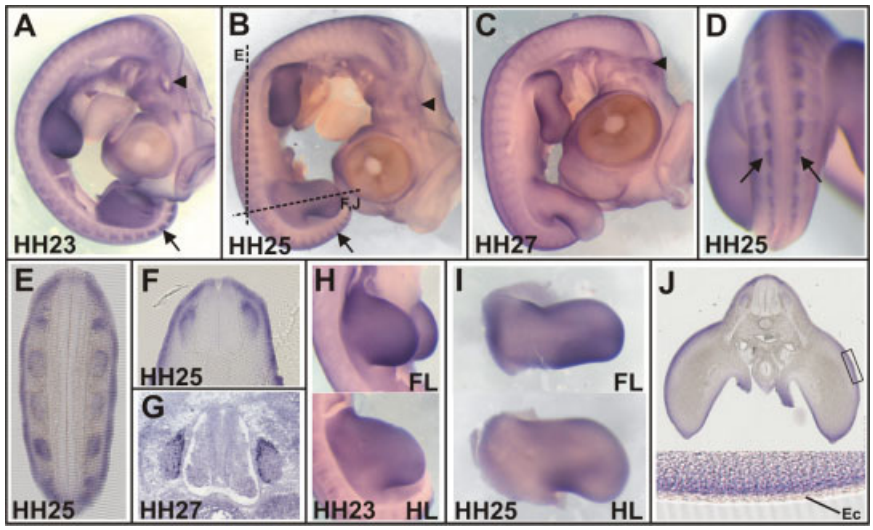

Fig. 2.

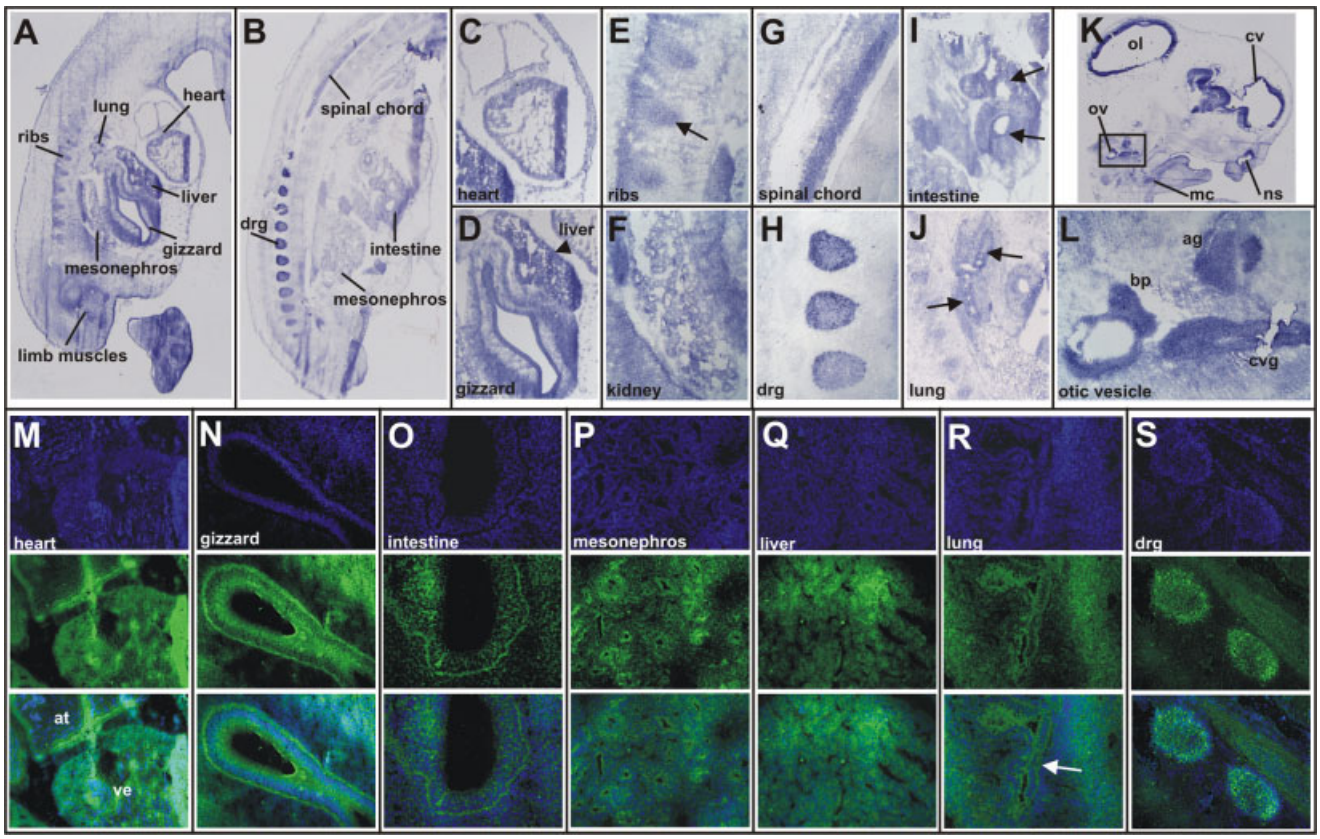

Fig. 3.

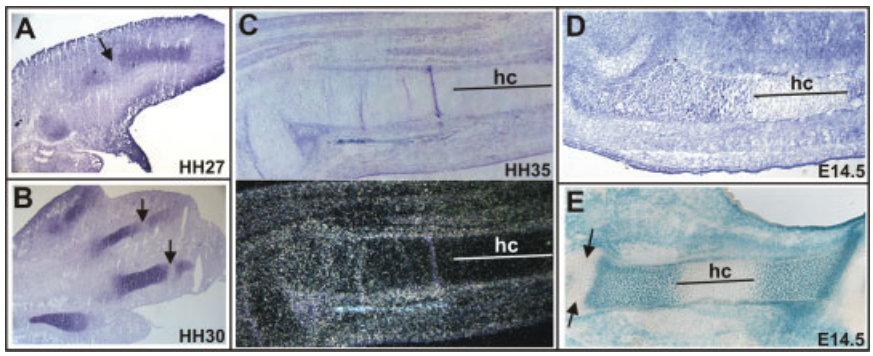

Fig. 4.

elements in zeugopod and stylopod was severely delayed, whereas the autopod was only mildly affected. In the proximal elements, ossification was strongly delayed or completely prevented at HH37, indicating a delay/block in chondrocyte differentiation. Infection with the most proximal BDB truncation (R433X) resulted in a reproducibly weaker phenotype when compared with the other BDB mutants and also the RS mutant Q494X.

BDB is a dominant condition. It was thus speculated that the truncating mutations causing BDB act as dominant-negatives, whereas RS is most likely to be caused by loss of protein function (Schwabe et al., 2000, 2004). However, in our experimental system, the RS mutation Q494X causes a phenotype comparable to the BDB mutants, albeit weaker than the E459X and 1374insA mutations.

Of interest, all human mutations leading to BDB that truncate ROR2 before the TK domain are frameshift mutations. This finding raises the possibility that the presence of an additional C-terminal peptide might have an influence on the pathogenic role of ROR2. We, therefore, fused the human frameshift mutation 1398insA (Schwabe et al., 2000) to the proximal part of chicken Ror2 at the identical position (1374; see Fig. 5). As described above, overexpression of this construct showed an identical result as overexpression of the variant E459X, which is truncated at the same position. Most strikingly, a brachydactyly phenotype was never observed (Fig. 6B). The smaller size and the delay in ossification observed in the autopod cartilage elements indicated viral infection in this area, thus excluding lack of viral spread in the autopod. In all cases, a mesomelic shortening of cartilaginous elements with delay/block of ossification was

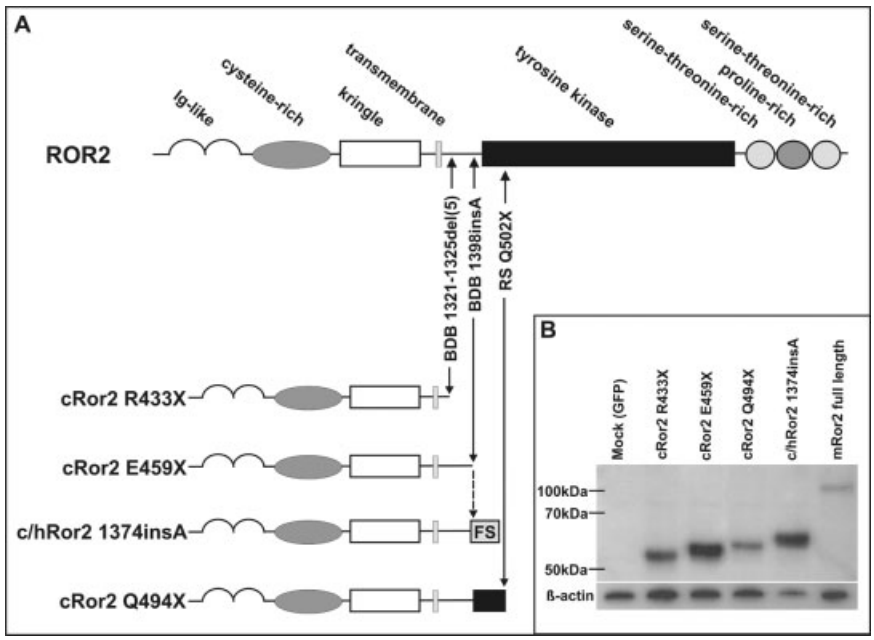

Fig. 5. Schematic depiction of the different cRor2 mutants used for replication-competent retroviral vector–mediated overexpression. **A:** Constructs were generated corresponding to two different Brachydactyly type B (BDB) and one Robinow syndrome (RS) mutation, respectively. Chicken Ror2 R433X and E459X truncate the protein at positions corresponding to frameshifts/stops set by the BDB mutations 1321-1325del(5) and 1398insA. A heterologous construct was generated, in which the human frameshift (FS) caused by the 1398insA mutation was fused to the proximal part of cRor2, thus exactly copying the BDB mutation (c/hRor2 1374insA, gray box). As a construct corresponding to a Robinow syndrome mutation (Q502X), a stop mutation was introduced at the corresponding position 494 in the chick. **B:** Protein expression from all four viral constructs used in this study and green fluorescent protein (GFP) -control virus in DF1 cells. As positive control, protein extract from HEK293 cells transfected with mouse Ror2 full-length was used (right lane). β-actin was used as a loading control.

Fig. 2. Expression of *cRor2* in whole chick embryos. Hamburger and Hamilton (HH) stages are indicated. **A–D:** Whole-mount in situ hybridization (ISH) showing expression of *cRor2* in craniofacial mesenchyme, branchial arches, otic vesicle (arrowheads), dorsal root ganglia (drg, arrows), and limbs. **H,I:** Magnification of forelimbs (FL) and hindlimbs (HL) from stages 23 and 25 are shown. **E,F:** Vibratome sections from HH25 embryos hybridized with *cRor2* in planes as indicated by dotted lines in B. **G:** Section ISH showing signal in drg. **J:** Vibratome section demonstrating *cRor2* expression in superficial mesenchymal cell layers in the limb; ectoderm shows no expression (boxed region shown as magnification below). Ec, ectoderm.

Fig. 3. Expression of cRor2 mRNA and protein on sections from Hamburger and Hamilton stage (HH) 29 chicken embryos. A–L: In situ hybridizations. M–S: Immunohistochemistry. **A,B:** Sagittal and parasagittal sections, respectively, giving an anatomical overview as well as an overview of *cRor2* expression. **C–J:** Magnification of sections shown in A,B show expression of *cRor2* in the heart (C), gizzard and liver (D, arrowhead), rib condensations (E, arrow), mesonephros (F), spinal chord (G), dorsal root ganglia (H), intestinal loops (I, arrows), and lung (J, arrows). **K:** *cRor2* expression in the head. **L:** Magnification from the boxed area in K. **M–S:** Immunohistochemistry on cryosections adjacent to those shown in A,B confirms expression of cRor2 in the heart (M), gizzard (N), intestine (O), mesonephros (P), liver (Q), lung (R), and dorsal root ganglia and spinal chord (S). ag, acoustic ganglion; at, atrium; bp, basilar papilla; cv, cerebral vesicle; cvg, cochleovestibular ganglion; drg, dorsal root ganglia; mc, Meckel's cartilage; ns, nasal sac; ol, optic lobe; ov, otic vesicle; ve, ventricle.

Fig. 4. Expression of *cRor2* in the developing limb cartilage. **A:** At Hamburger and Hamilton stage (HH) 27, *cRor2* can be detected in the condensations of the proximal limb cartilage elements. **B:** At HH30, expression can be seen in the condensations of the phalanges. Presumptive joints are excluded (arrows). **C:** In the tibia growth plate at HH35, *cRor2* is expressed in undifferentiated, nonhypertrophic chondrocytes and in the perichondrium as determined by radioactive in situ hybridization. Top: Brightfield picture of section stained with toluidine blue. Bottom: Darkfield image. **D,E:** A similar pattern was found in the mouse by in situ hybridization (D) and beta-galactosidase staining on limbs from $Ror2^{lacZ/+}$ embryos (E). Note absence of beta-galactosidase staining in joint region (arrows). Hc, hypertrophic chondrocytes.

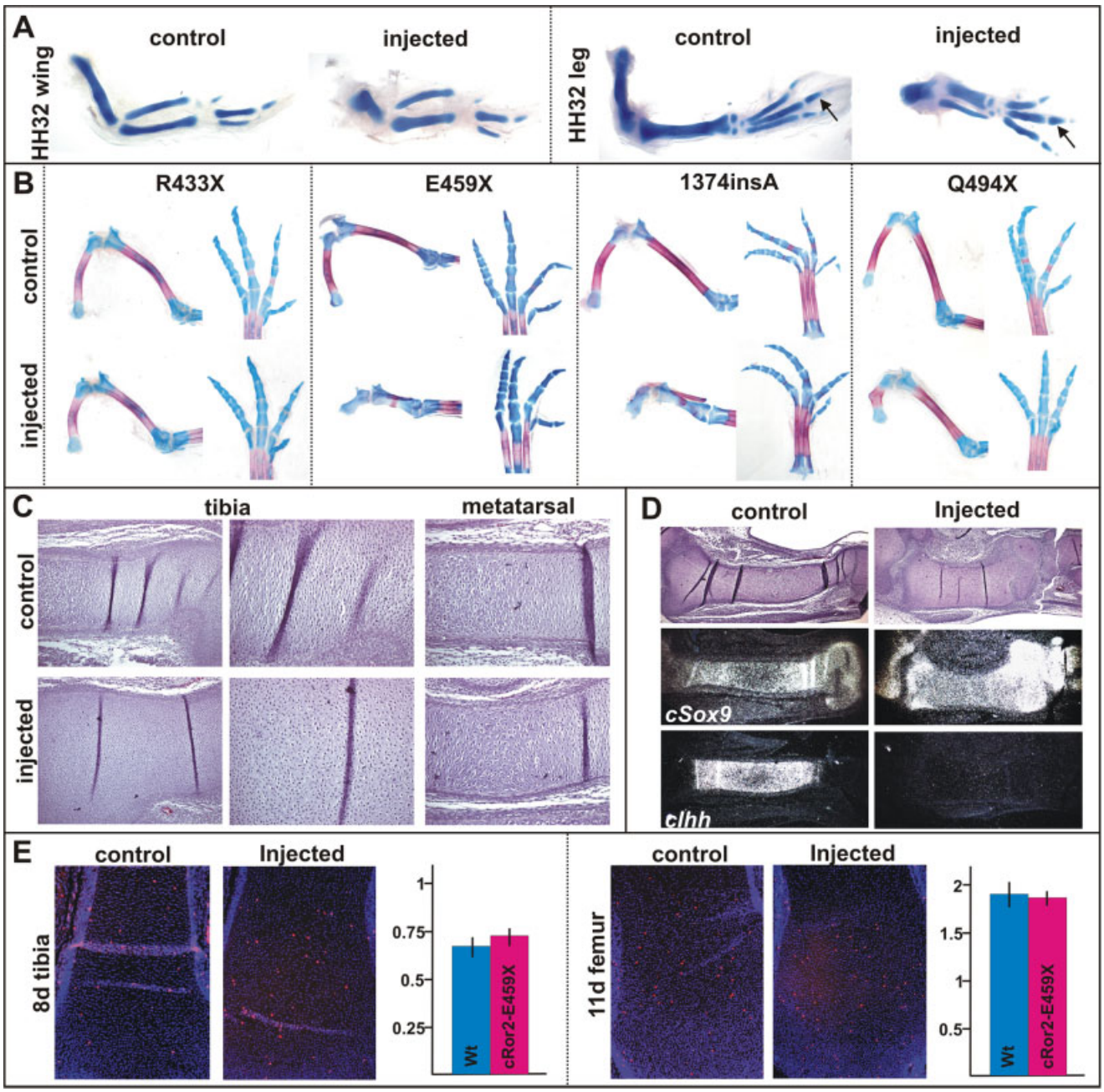

Fig. 6. Consequences of overexpression of different cRor2 mutants in vivo. **A:** Representative data demonstrating the effect of cRor2-E459X overexpression in chicken fore- and hindlimbs. Limbs were harvested after 7.5 days of development (Hamburger and Hamilton stage [HH] 32), the limb skeleton is stained with Alcian blue. Note the shorter and thicker appearance of distal condensations (arrows). **B:** Comparison of overexpression phenotypes caused by the different mutations. Limbs were harvested after 11 days (HH37) and stained with Alcian blue and alizarin red. Note the absence of a brachydactyly phenotype in all cases. **C:** Hematoxylin and eosin–stained sections through tibia and metatarsal of HH32 injected and control limbs. Note the lack of flattened chondrocytes in the infected tibia and the disarrayed growth plate in the metatarsal. **D:** In situ hybridization with *cSox9* and *cIhh* on tibia sections of HH32 injected and control limbs, demonstrating a block in chondrocyte differentiation. **E:** Unchanged proliferation rate (Histone-H3 labeling) on strongly affected HH32 tibia and mildly affected HH37 femur versus contralateral controls. Nuclei are stained with 4′,6-diamidine-2-phenylidole-dihydrochloride (DAPI, blue), Histone-H3 is stained with Alexa Fluor 568 (red). Proliferation rate was assessed as percentage of Histone-H3–stained nuclei relative to DAPI-stained nuclei within the growth plate. Columns represent mean values from eight different sections. Error bars represent standard deviations. The differences are insignificant as determined by Student's *t*-test ($P > 0.2$).

seen. Thus none of the BDB constructs, although the 1374insA variant was bearing an exact copy of the human mutation 1398insA, was able to phenocopy the human phenotype. A possible explanation might be that the observed discrepancies are due to species differences. In humans, BDB is a dominant condition characterized by missing medial and distal phalanges, but the respective mouse model (DeChiara et al., 2000) shows a considerably milder phenotype with missing medial phalanges, which is penetrant only in the homozygous

condition. This condition might be one example where the human limb is more susceptible to alterations in signaling balances than the mouse or the chick. Similar findings have recently been reported for loss-of-function mutations in Wnt7a, which cause mild dorsoventral polarity phenotypes in the mouse (Parr and McMahon, 1995), but in humans WNT7A loss of function causes a range of severe limb malformation syndromes (Woods et al., 2006).

Truncated Forms of Ror2 Delay Chondrocyte Differentiation

Once initial cartilaginous condensations are formed, a fine balance of chondrocyte proliferation and differentiation controls the growth of the skeletal elements. As shown before, after overexpression in vivo, the BDB mutant E459X and 1374insA displayed the strongest phenotype. Thus subsequent experiments were performed with the construct E459X. Hematoxylin and eosin–stained sections from infected and control tibia at HH32 demonstrate presence of small, rounded chondrocytes throughout the infected cartilage element, whereas the control tibia shows the normal chicken growth plate array of undifferentiated, flattened, and hypertrophic chondrocytes (Fig. 6C). In the metatarsal bones, where the skeletal preparations had generally shown a milder phenotype, some degree of chondrocyte differentiation occurred. However, the normal growth plate architecture was severely disturbed (Fig. 6C). The undifferentiated appearance of chondrocytes after overexpression of cRor2-E459X was confirmed by in situ hybridization for *cSox9*, a marker for early chondrocytes. In the wild-type, the diaphysial region shows no expression of *cSox9*, whereas in the infected limb, *cSox9* was expressed throughout the cartilage (Fig. 6D). Conversely, the wild-type tibia shows strong expression of *cIhh*, a marker for prehypertrophic chondrocytes (Vortkamp et al., 1996), which is completely lacking in the infected tibia (Fig. 6D). Again, in the metatarsals, the delay of differentiation is less pronounced. Expression of *cIhh* occurs in infected elements, however, it is markedly down-regulated (not shown). Thus truncated Ror2 appears to severely disrupt growth plate architecture and chondrocyte differentiation at or before the onset of prehypertrophic differentiation.

To analyze alterations in chondrocyte proliferation, we performed phospho-Histone-H3 labeling (Galli et al., 2004) on sections of infected and control limbs. We applied this method to the severely affected tibias infected with the E459X mutant used above and also to femurs of less severe affected embryos, which were significantly shortened (40%), but still showed an intact growth plate morphology. As demonstrated in Figure 6E, we did not observe differences in chondrocyte proliferation in either case.

Taken together, the overexpression of truncated forms of cRor2 led to a severe defect in cartilage differentiation, predominantly in the proximal elements, without affecting proliferation. This finding is in agreement with previous findings in the Ror2 null mouse, where Schwabe et al. (2004) ascribed the mesomelic limb shortening to a defect in chondrocyte differentiation but not proliferation. Thus the effect we observed after overexpression of BDB mutants mirrors a loss of function of Ror2, which could be explained by a dominant-negative action of the mutant constructs over the endogenous protein. However, the phenotype we observed is stronger than in $Ror2^{-/-}$ embryos. This observation indicates that also other pathways may be negatively influenced. Of interest, double knockout of Ror2 and Ror1 increases the phenotypic severity to a level comparable with our chicken experiments (Nomi et al., 2001), indicating that mutant Ror2 constructs might also interfere with Ror1 signaling. In addition, other pathways could be influenced by the mutant constructs. There is growing evidence that Ror2 can interact with several of the Wnt signaling factors (Hikasa et al., 2002; Oishi et al., 2003; Billiard et al., 2005). Recently it was shown that Ror2 can act as a coreceptor for Wnt5a, thereby leading to inhibition of canonical Wnt signaling (Mikels and Nusse, 2006). Moreover, it was shown previously, that Ror2 can also interact with and inhibit the bone morphogenetic protein-receptor type 1b (BmpR1b) pathway, an activity lost in truncated Ror2-mutants (Sammar et al., 2004). Interestingly, both Bmp and Wnt/beta-catenin pathways can interact on different levels in a variety of processes (Hoffmann and Gross, 2001, and references therein; Church and Francis-West, 2002; Grotewold and Ruther, 2002; Hartmann, 2006). This might implicate Ror2 at a central position in a regulatory network integrating distinct pathways by modulating their activity and potentially also their cross-talk. It will be a challenging task to elucidate the relationships of Ror2 and the different aspects of canonical and noncanonical Wnt signaling as well as Bmp signaling.

EXPERIMENTAL PROCEDURES

Cloning of *cRor2*

We derived 222 bp of the 3′ coding sequence and the partial 3′ untranslated region (UTR) from chicken EST 369c3 obtained from the BBSRC (Boardman et al., 2002). Briefly, exon 9 of *cRor2* containing the entire tyrosine kinase domain was cloned by genomic walking. Sequence encoded by exons 2–8 was cloned by PCR from 5-day-old chick embryo cDNA using degenerate nested 5′ primers. The 5′ end of the coding sequence and part of the 5′ UTR were determined by 5′ RACE (Clontech SMART-RACE kit). Detailed protocols and primer information are available upon request. The coding sequence of *cRor2* has been deposited in GenBank EF017720.

In Situ Hybridization and Immunohistochemistry

For ISH we used two different probes. A PCR-generated probe (F: TGGTATCAACGCAGAGTACG, R: GGAGCACTGCGGCGACAAGC) comprised a part of the 5′ UTR and part of the 5′ cds. The PCR fragment was cloned into pCRII-TOPO (Invitrogen), linearized with *Hin*dIII, and transcribed with T7. A second probe was generated from pSlax13/cRor2-E459X by linearization with *Nco*I and transcription with T7. Both probes yielded identical results. Whole-mount ISH was carried out as described in

Schwabe et al. (2004). Section ISH was carried out as follows: cryosections were air-dried, fixed in paraformaldehyde for 10 min, acetylated for 10 min, and then hybridized overnight at 70°C. Slides were then washed two times for 30 min at 65°C with 0.2× standard saline citrate, blocked in 10% goat serum, followed by incubation with anti–digoxigenin-alkaline phosphatase (Roche) in 10% goat serum overnight at 4°C. Staining was performed with nitroblue tetrazolium/5-bromo-4-chloro-3-indolyl phosphate (NBT/BCIP; Roche) according to the manufacturer's recommendations. Radioactive ^{33}P-labeled ISH was carried out as in Stricker et al. (2002).

Immunohistochemistry for cRor2 was performed on fresh frozen sections. After thawing, fixation was done 10 min with ice-cold methanol at −20°C, followed by washing with PBS. Permeabilization was done for 10 min with 3% fetal calf serum (FCS)/0.1% saponin in phosphate buffered saline (PBS). After washing, sections were blocked in 10% FCS in PBS overnight. The next day, the primary antibody (R&D Systems anti-human ROR2, 1:50) was applied in 5% FCS in PBS and incubated overnight at 4°C. After several washing steps, the sections were incubated with secondary antibody (anti-goat Alexa Fluor 488, Molecular Probes, 1:1,000 in 5% FCS/PBS) and 4′,6-diamidine-2-phenylidole-dihydrochloride (DAPI; 1:2,000) for 1 hr at room temperature. Finally, after washing in PBS, the sections were mounted in Fluoromount and analyzed with a Axiovert-200 fluorescence microscope (Zeiss). As a negative control, secondary antibody was applied without prior incubation with anti-ROR2.

Phospho-Histone-H3 labeling was performed on paraffin sections. Sections were deparaffinized, rehydrated, and boiled for 10 min in 0.01 M sodium citrate pH 6.0. Anti-phospho-Histone-H3 (Upstate) was applied in 0.1% bovine serum albumin in PBS at 1:200 overnight in a humidified chamber at 4°C. Slides were washed in PBS, and secondary antibody (anti-rabbit Alexa Fluor 568, Molecular Probes) was applied in 10% FCS in PBS at 1:500 for 1 hr. DAPI (Roche) was added to this solution at 1:2,000. After washing in PBS, slides were mounted in Fluoromount.

Western Blotting

To detect different Ror2 constructs, 20 μg of lysate of RCAS-infected DF1 cells or HEK293 cells transfected with full-length mRor2 were run on a 12% sodium dodecyl sulphate-polyacrylamide gel electrophoresis and blotted to nylon membrane according to standard procedures. Ror2 protein was detected with anti-human-ROR2 antibody recognizing the extracellular part of Ror2 (R&D Systems, 1:1,000).

Cloning of *cRor2* Constructs, Virus Production, and Overexpression

The truncating mutations R433X, E459X, and Q494X were generated by PCR on chicken embryo HH27 cDNA using the primers F-Nco, ATACCATGGTCCCCGCGGCCGCTCTGCGTCTC and R-433, ATAGAATTCTCACTGTGGTGTGGTGGCAGATGC; R-459, ATAGAATTCTTATTTAAGTTTAGTCTGTTTGTGTTG; R-494, ATAGAATTCTCATTGTGTTTGTTCACCTGGTGCAGTACC. The 1374insA fusion construct was obtained as follows: first, the human frameshift part was amplified from HEK293 cDNA with primers F, CCACTCATTAATCAACACAAACAGACTAAACTTAAAAGAGATCAGCCTGTCTGCGGTGAG (inserted A underlined); R, ATGAATTCTCATGCCGGAACTCCTCCCGCAG. Then this PCR product was used as reverse primer in a fusion PCR on chicken cDNA together with forward primer F-Nco (see above). All constructs were cloned to pSlax13 by means of *Nco*I and *Eco*RI. Constructs were shuttled from pSlax13 to RCAS(BP)A by means of *Cla*I. Production of viral supernatant in DF1 cells and concentration of viral particles was performed as described in Morgan and Fekete (1996). All preparations used had a viral titer of at least 5×10^8 infectious units per milliliter. Injection of concentrated virus into HH10 chick embryo limb fields was performed as described in Logan and Tabin (1998).

ACKNOWLEDGMENTS

S.M. and S.S. were funded by the Deutsche Forschungsgemeinschaft.

REFERENCES

Afzal AR, Rajab A, Fenske CD, Oldridge M, Elanko N, Ternes-Pereira E, Tuysuz B, Murday VA, Patton MA, Wilkie AO, Jeffery S. 2000. Recessive Robinow syndrome, allelic to dominant brachydactyly type B, is caused by mutation of ROR2. Nat Genet 25:419–422.

Al-Shawi R, Ashton SV, Underwood C, Simons JP. 2001. Expression of the Ror1 and Ror2 receptor tyrosine kinase genes during mouse development. Dev Genes Evol 211:161–171.

Billiard J, Way DS, Seestaller-Wehr LM, Moran RA, Mangine A, Bodine PV. 2005. The orphan receptor tyrosine kinase Ror2 modulates canonical Wnt signaling in osteoblastic cells. Mol Endocrinol 19:90–101.

Boardman PE, Sanz-Ezquerro J, Overton IM, Burt DW, Bosch E, Fong WT, Tickle C, Brown WR, Wilson SA, Hubbard SJ. 2002. A comprehensive collection of chicken cDNAs. Curr Biol 12:1965–1969.

Chen Y, Bellamy WP, Seabra MC, Field MC, Ali BR. 2005. ER-associated protein degradation is a common mechanism underpinning numerous monogenic diseases including Robinow syndrome. Hum Mol Genet 14:2559–2569.

Church VL, Francis-West P. 2002. Wnt signalling during limb development. Int J Dev Biol 46:927–936.

DeChiara TM, Kimble RB, Poueymirou WT, Rojas J, Masiakowski P, Valenzuela DM, Yancopoulos GD. 2000. Ror2, encoding a receptor-like tyrosine kinase, is required for cartilage and growth plate development. Nat Genet 24:271–274.

Forrester WC, Dell M, Perens E, Garriga G. 1999. A C. elegans Ror receptor tyrosine kinase regulates cell motility and asymmetric cell division. Nature 400:881–885.

Galli LM, Willert K, Nusse R, Yablonka-Reuveni Z, Nohno T, Denetclaw W, Burrus LW. 2004. A proliferative role for Wnt-3a in chick somites. Dev Biol 269:489–504.

Grotewold L, Ruther U. 2002. Bmp, Fgf and Wnt signalling in programmed cell death and chondrogenesis during vertebrate limb development: the role of Dickkopf-1. Int J Dev Biol 46:943–947.

Hartmann C. 2006. A Wnt canon orchestrating osteoblastogenesis. Trends Cell Biol 16:151–158.

Hikasa H, Shibata M, Hiratani I, Taira M. 2002. The Xenopus receptor tyrosine kinase Xror2 modulates morphogenetic movements of the axial mesoderm and neuroectoderm via Wnt signaling. Development 129:5227–5239.

Hoffmann A, Gross G. 2001. BMP signaling pathways in cartilage and bone formation. Crit Rev Eukaryot Gene Expr 11:23–45.

Katoh M, Katoh M. 2005. Identification and characterization of rat Ror1 and Ror2 genes in silico. Int J Mol Med 15: 533–538.

Logan M, Tabin C. 1998. Targeted gene misexpression in chick limb buds using avian replication-competent retroviruses. Methods 14:407–420.

Masiakowski P, Carroll RD. 1992. A novel family of cell surface receptors with tyrosine kinase-like domain. J Biol Chem 267:26181–26190.

Matsuda T, Nomi M, Ikeya M, Kani S, Oishi I, Terashima T, Takada S, Minami Y. 2001. Expression of the receptor tyrosine kinase genes, Ror1 and Ror2, during mouse development. Mech Dev 105: 153–156.

McKay SE, Hislop J, Scott D, Bulloch AG, Kaczmarek LK, Carew TJ, Sossin WS. 2001. Aplysia ror forms clusters on the surface of identified neuroendocrine cells. Mol Cell Neurosci 17:821–841.

Mikels AJ, Nusse R. 2006. Purified Wnt5a protein activates or inhibits beta-catenin-TCF signaling depending on receptor context. PLoS Biol 4:e115.

Morgan BA, Fekete DM. 1996. Manipulating gene expression with replication-competent retroviruses. Methods Cell Biol 51:185–218.

Nomi M, Oishi I, Kani S, Suzuki H, Matsuda T, Yoda A, Kitamura M, Itoh K, Takeuchi S, Takeda K, Akira S, Ikeya M, Takada S, Minami Y. 2001. Loss of mRor1 enhances the heart and skeletal abnormalities in mRor2-deficient mice: redundant and pleiotropic functions of mRor1 and mRor2 receptor tyrosine kinases. Mol Cell Biol 21:8329–8335.

Oishi I, Sugiyama S, Liu ZJ, Yamamura H, Nishida Y, Minami Y. 1997. A novel Drosophila receptor tyrosine kinase expressed specifically in the nervous system. Unique structural features and implication in developmental signaling. J Biol Chem 272:11916–11923.

Oishi I, Takeuchi S, Hashimoto R, Nagabukuro A, Ueda T, Liu ZJ, Hatta T, Akira S, Matsuda Y, Yamamura H, Otani H, Minami Y. 1999. Spatio-temporally regulated expression of receptor tyrosine kinases, mRor1, mRor2, during mouse development: implications in development and function of the nervous system. Genes Cells 4:41–56.

Oishi I, Suzuki H, Onishi N, Takada R, Kani S, Ohkawara B, Koshida I, Suzuki K, Yamada G, Schwabe GC, Mundlos S, Shibuya H, Takada S, Minami Y. 2003. The receptor tyrosine kinase Ror2 is involved in non-canonical Wnt5a/JNK signalling pathway. Genes Cells 8:645–654.

Oldridge M, Fortuna AM, Maringa M, Propping P, Mansour S, Pollitt C, DeChiara TM, Kimble RB, Valenzuela DM, Yancopoulos GD, Wilkie AO. 2000. Dominant mutations in ROR2, encoding an orphan receptor tyrosine kinase, cause brachydactyly type B. Nat Genet 24:275–278.

Parr BA, McMahon AP. 1995. Dorsalizing signal Wnt-7a required for normal polarity of D-V and A-P axes of mouse limb. Nature 374:350–353.

Patton MA, Afzal AR. 2002. Robinow syndrome. J Med Genet 39:305–310.

Saldanha J, Singh J, Mahadevan D. 1998. Identification of a Frizzled-like cysteine rich domain in the extracellular region of developmental receptor tyrosine kinases. Protein Sci 7:1632–1635.

Sammar M, Stricker S, Schwabe GC, Sieber C, Hartung A, Hanke M, Oishi I, Pohl J, Minami Y, Sebald W, Mundlos S, Knaus P. 2004. Modulation of GDF5/BRI-b signalling through interaction with the tyrosine kinase receptor Ror2. Genes Cells 9:1227–1238.

Schwabe GC, Tinschert S, Buschow C, Meinecke P, Wolff G, Gillessen-Kaesbach G, Oldridge M, Wilkie AO, Komec R, Mundlos S. 2000. Distinct mutations in the receptor tyrosine kinase gene ROR2 cause brachydactyly type B. Am J Hum Genet 67:822–831.

Schwabe GC, Trepczik B, Suring K, Brieske N, Tucker AS, Sharpe PT, Minami Y, Mundlos S. 2004. Ror2 knockout mouse as a model for the developmental pathology of autosomal recessive Robinow syndrome. Dev Dyn 229:400–410.

Stricker S, Fundele R, Vortkamp A, Mundlos S. 2002. Role of Runx genes in chondrocyte differentiation. Dev Biol 245:95–108.

Takeuchi S, Takeda K, Oishi I, Nomi M, Ikeya M, Itoh K, Tamura S, Ueda T, Hatta T, Otani H, Terashima T, Takada S, Yamamura H, Akira S, Minami Y. 2000. Mouse Ror2 receptor tyrosine kinase is required for the heart development and limb formation. Genes Cells 5:71–78.

Valenzuela DM, Stitt TN, DiStefano PS, Rojas E, Mattsson K, Compton DL, Nunez L, Park JS, Stark JL, Gies DR, et al. 1995. Receptor tyrosine kinase specific for the skeletal muscle lineage: expression in embryonic muscle, at the neuromuscular junction, and after injury. Neuron 15:573–584.

van Bokhoven H, Celli J, Kayserili H, van Beusekom E, Balci S, Brussel W, Skovby F, Kerr B, Percin EF, Akarsu N, Brunner HG. 2000. Mutation of the gene encoding the ROR2 tyrosine kinase causes autosomal recessive Robinow syndrome. Nat Genet 25:423–426.

Vortkamp A, Lee K, Lanske B, Segre GV, Kronenberg HM, Tabin CJ. 1996. Regulation of rate of cartilage differentiation by Indian hedgehog and PTH-related protein. Science 273:613–622.

Wilson C, Goberdhan DC, Steller H. 1993. Dror, a potential neurotrophic receptor gene, encodes a Drosophila homolog of the vertebrate Ror family of Trk-related receptor tyrosine kinases. Proc Natl Acad Sci U S A 90:7109–7113.

Woods CG, Stricker S, Seemann P, Stern R, Cox J, Sherridan E, Roberts E, Springell K, Scott S, Karbani G, Sharif SM, Toomes C, Bond J, Kumar D, Al-Gazali L, Mundlos S. 2006. Mutations in WNT7A cause a range of limb malformations, including Fuhrmann syndrome and Al-Awadi/Raas-Rothschild/Schinzel Phocomelia syndrome. Am J Hum Genet 79:402–408.